



Bergische Universität Wuppertal

Fachbereich Mathematik und Naturwissenschaften

Institute of Mathematical Modelling, Analysis and  
Computational Mathematics (IMACM)

Preprint BUW-IMACM 12/35

Michèle Wandelt, Michael Günther, Michael Striebel

**Symmetric, Time-Reversible and  
Volume-Preserving Projection Methods for  
Differential Equations on Manifolds: the  
Non-Abelian Case**

December 18, 2012

<http://www.math.uni-wuppertal.de>

# Symmetric, Time-Reversible and Volume-Preserving Projection Methods for Differential Equations on Manifolds: the Non-Abelian Case <sup>☆</sup>

Michèle Wandelt\*, Michael Günther\*, Michael Striebel\*

*Bergische Universität Wuppertal, Fachbereich Mathematik und Naturwissenschaften,  
D-42119 Wuppertal, Germany*

---

## Abstract

This work is concerned with symmetric and symplectic projection methods. The idea is based on symmetric projection schemes introduced by Hairer for ODE systems on a manifold in the Abelian case  $\mathbb{R}^n$ . These methods combine a symmetric scheme with a projection on the manifold, arising in an overall symmetric scheme which preserves the constraint defined by the manifold. We have generalized this scheme to projection schemes, which join a symmetric, time-reversible and symplectic scheme (Leapfrog, for example) with a projection on the manifold described by the Hamiltonian, resulting in a scheme with the aforementioned properties which preserves the Hamiltonian exactly. In a further step, we adapted the method to the non-Abelian case of matrix Lie groups to reduce the computational costs of Lattice QCD.

*Keywords:* Lie group methods, Projection methods, Geometric integrators, Lattice QCD

*2010 MSC:* 65P10, 65L05, 34C40, 70G65, 81T25

---

<sup>☆</sup>This research was supported by the Deutsche Forschungsgemeinschaft through the Collaborative Research Centre SFB-TR 55 “Hadron physics from Lattice QCD” and by the European Union under Grant Agreement number 238353 (ITN STRONGnet).

\*corresponding author

*Email addresses:* wandelt@math.uni-wuppertal.de (Michèle Wandelt),  
guenther@math.uni-wuppertal.de (Michael Günther), michael.striebe1@web.de  
(Michael Striebel)

*Preprint submitted to Journal of Computational and Applied Mathematics, December 18, 2012*

## 1. Introduction

Quantum Chromo Dynamics (QCD), the theory of strong interaction (or color force) between quarks and gluons inside subatomic particles, deals with the properties of elementary particles (hadrons) given by the expectation values  $\langle E \rangle$  of certain operators  $E$ . These expectations are needed to properly analyze experiments at the Large Hadron Collider (LHC) at CERN, for example, and are theoretically given by evaluating a high-dimensional path integral. As this integral can not be determined analytically, one has to rely on numerical simulation to sample the integral, resulting into Lattice QCD [1, 2]. One way of approximation in Lattice QCD is Hybrid Monte-Carlo: here samples are obtained by performing a molecular dynamics step in virtual time, applied to Hamiltonian equations of motion defined on a product space of Lie groups and associated Lie algebras. These samples are rejected with a probability proportionally to the defect in preserving the Hamiltonian. Hence, one is interested in numerical integration schemes approximating the Hamiltonian at high accuracy, which at the same time have to be volume-preserving and time-reversible to meet the detailed balance condition [3, 4]. Usually, one applies numerical geometric integration of preferably high order to meet these demands. For this purpose, the Leapfrog method, the Omelyan scheme [5, 6] or splitting methods with multiple timescales [7] according to Sexton-Weingarten are commonly used. Another approach would be the use of higher order symmetric partitioned Runge-Kutta methods described in [8]. In this paper, we will propose an alternative way: we will not use high order schemes to obtain a high accuracy in the Hamiltonian and, accordingly, a low rejection rate of the samples, but combine low order numerical geometric integration schemes with projection schemes which preserve the Hamiltonian exactly and, thus, avoid the rejection of samples.

The paper is organized as follows: in Section 2, we start with a motivation of time-reversible and volume-preserving projection methods for differential equations on manifolds arising from the non-Abelian case of Lattice QCD. In doing so, we give a short introduction in the field of Quantum Chromo Dynamics and Lattice QCD. The Hybrid Monte Carlo method used in Lattice QCD is explained in more detail including the necessary geometric properties of the molecular dynamics step to meet the detailed balance condition. In Section 3 we start from symmetric projection schemes [9] and develop time-reversible and volume-preserving projection schemes for the Abelian case. These results are generalized and applied to the non-Abelian case of Lattice

QCD in Section 4. Moreover, numerical results given in Section 5 for an SU(2) gauge field to verify the desired properties of our projection approach in the non-Abelian case of Lattice QCD. Finally, a conclusion and outlook to open question and future work is given in Section 6.

## 2. Motivation: Lattice QCD and numerical geometric integration

In Lattice QCD, the approximation of expectation values needed in QCD is usually performed on a 4-dimensional space-time lattice consisting of elementary particles  $U$ . The field configuration  $\{U\}$  is composed of all particles  $U$  on the lattice. Expectation values  $\langle E \rangle$  are computed by summing up a selected ensemble of field configurations  $\{U\}$ . Since the contribution of nearly all configurations is very small, one decreases the computational effort by preferring configurations  $\{U^i\}$  occurring with a high probability  $p_i$ :

$$\langle E \rangle = \sum_{\{U^i\}} p_i \cdot E(\{U^i\}). \quad (1)$$

This approach is realized in the Metropolis Monte Carlo method, which uses a Markov chain process to generate new field configurations which should reach the equilibrium distribution (i.e. the fixed point of the Markov process) at the end. In doing so, a new configuration  $\{U^j\}$  is created randomly and afterwards accepted with a certain transition probability  $T_{ij} := \min(1, \frac{p_j}{p_i})$  to reach configuration  $\{U^j\}$  from  $\{U^i\}$ . Thereby, the so-called detailed balance condition concerning the action  $S(\{U\})$ , i. e.

$$p_i T_{ij} = p_j T_{ji} \quad \text{with} \quad p_i \sim \exp(-S(\{U^i\})). \quad (2)$$

with probability  $p_i$  to find configuration  $\{U^i\}$  has to be fulfilled to reach the fixed point of the Markov process.

### 2.1. HMC Algorithm and Molecular Dynamics Step

This approach can be improved by the Hybrid Monte Carlo (HMC) method, a type of Markov Chain Monte Carlo (MCMC) method published by Duane et al. [3] in 1987.

The idea is to use a Hamiltonian  $H_i := H\{U^i, P^i\}$  (which is a constant in time) for the probability distribution  $p_i = \exp(-H_i)$  to achieve a high acceptance rate. To obtain the Hamiltonian equations of motion, a fictitious time and a field of fictitious momenta  $\{P\}$  are introduced. Here, one starts with

an initial configuration  $\{U^i, P^i\}$  at time  $t = 0$  and gets the new configuration  $\{U^j, P^j\}$  by applying a Molecular Dynamics step. Due to the fact that the Hamiltonian is conserved in time, the Hamiltonians of two successive configurations will be the same up to the numerical errors of the integration method. As the transition probability

$$T_{ij} := \min(1, \frac{p_i}{p_j}) = \min(1, \exp(-\Delta H)) , \Delta H := H_i - H_j$$

depends only on the difference of the Hamiltonians  $\Delta H$ , the acceptance rate is linked to the convergence order of the numerical integration scheme used in the Molecular Dynamics step.

It is essential for the Hybrid Monte Carlo method that the Markov process converges to the fixed point of the equilibrium distribution of the field configurations  $\{U\}$ . To ensure this, the numerical integration scheme still has to fulfill the detailed balance condition (2) concerning the action  $S(\{U\})$ . Therefore, the numerical integration schemes used in the Molecular Dynamics Step have to be time-reversible and should be volume-preserving. The time-reversibility is mandatory, while a missing volume-preservation can be compensated theoretically by a proper scaling with the determinant of the Jacobian of the whole system  $\partial\{U^j, P^j\}/\partial\{U^i, P^i\}$ .

The convergence order  $p$  of the numerical integration scheme is just of interest to achieve a high acceptance rate because  $|\Delta H|$  is proportional to the error of the integration scheme.

## 2.2. Projection Schemes

Our aim is the development of projection schemes for the Molecular Dynamics Step of the Hybrid Monte Carlo method. For this purpose, the projection scheme has to fulfill several properties:

- first of all, it has to be time-reversible to reach the correct fixed point of the Markov chain;
- then, it should be volume-preserving; otherwise the Jacobian of a system of huge dimension has to be computed;
- additionally, the Hamiltonian should remain constant.

If all these demands are met, one gets an overall time-reversible, volume-preserving projection scheme that preserves the Hamiltonian. It has the following advantages: the acceptance step can be dropped because  $\Delta H = 0$ ;

there is no need for higher order methods or small step sizes, one large integration step is sufficient.

In a first step, we will construct such schemes for the Abelian case.

### 3. Projection Schemes for the Abelian Case

Symmetric projection schemes have been introduced by Hairer [9] to solve numerically the initial value problem

$$y' = f(y), \quad y(0) = y_0$$

in the Abelian case  $y \in \mathbb{R}^{2n}$  subject to an invariant manifold defined by a constraint  $g(y) = 0$ . These schemes combine one step of a symmetric integration method  $\Phi_h$  with a symmetric forward and backward projection to obtain a symmetrical method and at the same time to preserve the constraint: first of all, the initial value  $y_0$  is perturbed orthogonal to the manifold:

$$P_f^\mu : \quad \tilde{y}_0 = y_0 + G^\top(y_0)\mu$$

with  $G^\top(y)$  denoting the Jacobian of  $g(y)$ . After that, one symmetric numerical integration step is performed:

$$\Phi_h : \quad \tilde{y}_1 = \Phi_h(\tilde{y}_0).$$

Finally, the result is projected back to the manifold:

$$P_b^\mu : \quad y_1 = \tilde{y}_1 + G^\top(y_1)\mu.$$

Here, the perturbation  $P_f^\mu$  and projection step  $P_b^\mu$  depend on a parameter  $\mu$  that is implicitly defined by the constraint  $g(y) = 0$ .

Our aim is to adapt the symmetric projection method to a simple time-reversible and volume-preserving projection scheme in the case of general Hamiltonian equations of motion given by

$$y' = f(y) = J^{-1}\nabla H(y) \quad \text{with} \quad y = (q, p)^\top, \quad J = \begin{pmatrix} 0 & I \\ -I & 0 \end{pmatrix},$$

initial values  $y(0) = y_0$  and the energy-preserving constraint

$$g(y) = H(y) - H(y_0) = 0.$$

Note that – in contrast to [9] – we regard the projection parameter  $\mu$  as variable, but fixed, thus yielding a parametrized family of numerical approximations  $y_h^\mu$  for step size  $h$ . At the end, we are interested in the scheme  $y_h^{\mu_{opt}}$  defined by

$$g(y_h^{\mu_{opt}}) = H(y_h^{\mu_{opt}}) - H(y_0) = 0.$$

The aforementioned adaption can be realized by three steps:

1. replace the symmetric integration method with a symmetric and at the same time time-reversible and volume-preserving one;
2. next, ensure that the overall scheme is volume-preserving;
3. and after all, make the overall scheme time-reversible.

The first step is very similar to the symmetric projection and can be realized, for example, by use of the Leapfrog integration scheme or the implicit midpoint rule as described in [10]. The new scheme

$$\Psi_h^\mu := P_b^\mu \circ \Phi_h \circ P_f^\mu. \quad (3)$$

is still symmetric, but in general neither volume-preserving nor time-reversible.

### 3.1. Volume-Preservation

The volume is preserved, if

$$|\det(D\Psi_h^\mu(y_0))| = 1 \quad \text{with} \quad D\Psi_h^\mu(y) := \frac{\partial \Psi_h^\mu(y)}{\partial y}$$

holds, i. e., it has to be checked whether the modulus of the determinant of the Jacobian is equal 1. Since the result  $y_1 = \Psi_h^\mu(y_0)$  is computed in three steps, a short computation shows that the method is in general not volume-preserving because the determinant of the Jacobian reads

$$\begin{aligned} |\det D\Psi_h^\mu(y_0)| &= \left| \det \left( DP_b^\mu(y) \Big|_{y=(\Phi_h \circ P_f^\mu)(y_0)} \cdot D\Phi_h(y) \Big|_{y=P_f^\mu(y_0)} \cdot DP_f^\mu(y_0) \right) \right| \\ &= \left| \det \left( I - DG^\top(y_1)\mu \right)^{-1} \cdot \det \left( I + DG^\top(y_0)\mu \right) \right| \end{aligned}$$

and is usually not equal to 1. Nevertheless, there is a simple way to ensure the volume-preservation: first of all, replace the matrix  $DG^\top(y)$  by a constant

matrix  $A^\top$  such that the projection matrix  $G^\top(y)$  is replaced by  $A^\top \cdot y$ . In doing so, the modulus of the determinant of the Jacobian reads

$$|\det D\Psi_h^\mu(y_0)| = |\det(I - A^\top \mu)^{-1} \cdot \det(I + A^\top \mu)|;$$

but, unfortunately, the modulus of the determinant will again not be equal to 1 in general. There has to be an additional sign flip in either the forward or the backward projection to achieve this. A sign flip in the backward projection gives the overall system

$$\begin{aligned} P_f^\mu : & \quad \tilde{y}_0 = y_0 + A^\top y_0 \mu \\ \Phi_h : & \quad \tilde{y}_1 = \Phi_h(\tilde{y}_0) \\ P_b^\mu : & \quad y_1 = \tilde{y}_1 - A^\top y_1 \mu, \quad \mu : H \text{ constant.} \end{aligned} \tag{4}$$

Using the short-hand notation  $\Psi_h^\mu$  defined in (3), we get

$$|\det D\Psi_h^\mu(y_0)| = |\det(I + A^\top \mu)^{-1} \cdot \det(I + A^\top \mu)| = 1$$

and thus, the method given in (4) is volume-preserving. At this point, it can be easily checked that the adapted method is still symmetric and even symplectic.

### 3.2. Time-Reversibility

So far, we have a symmetric and symplectic projection scheme given in (4). It is essential, that the scheme is also time-reversible, i. e., the condition

$$\rho \circ \Psi_h^\mu = (\rho \circ \Psi_h^\mu)^{-1} \quad \text{with} \quad \rho = \begin{pmatrix} I & 0 \\ 0 & -I \end{pmatrix} \tag{5}$$

consisting of blocks of size  $n \times n$  has to be fulfilled. The overall system reads

$$\Psi_h^\mu(y) = (I + A^\top \mu)^{-1} \cdot \Phi_h\left((I + A^\top \mu)(y)\right) \tag{6}$$

and with the time-reversibility of the inner one-step scheme  $\Phi_h$  it can be shown that it is sufficient to choose a matrix  $A$  with block-diagonal structure according to the dimensions of  $q$  and  $p$  of  $y = (q, p)^\top$ .

*Proof:* for

$$\Psi_h^\mu = B_\mu^{-1} \cdot \Phi_h \cdot B_\mu \quad \text{with} \quad B_\mu := I + A^\top \mu.$$

we have to verify the condition for time-reversibility

$$\rho \Psi_h^\mu = (\rho \Psi_h^\mu)^{-1} \quad \Leftrightarrow \quad \rho \cdot \Psi_h^\mu \cdot \rho \cdot \Psi_h^\mu = id,$$

or equivalently,

$$\rho \cdot B_\mu^{-1} \cdot \Phi_h \cdot B_\mu \cdot \rho \cdot B_\mu^{-1} \cdot \Phi_h \cdot B_\mu \stackrel{!}{=} id.$$

Using the time-reversibility of  $\Phi_h$  and the fact that  $\rho$  is idempotent, we can replace one of the one-step schemes  $\phi_h$  with  $\rho \cdot \Phi_h^{-1} \cdot \rho$  and get

$$id \stackrel{!}{=} \rho \cdot B_\mu^{-1} \cdot \Phi_h \cdot (B_\mu \cdot \rho \cdot B_\mu^{-1} \cdot \rho) \cdot \Phi_h^{-1} \cdot \rho \cdot B_\mu.$$

If we assume  $B_\mu \cdot \rho \cdot B_\mu^{-1} \cdot \rho = id$  we are done. A sufficient but not necessary condition would be that the matrix  $B_\mu$ , respective  $A$ , is block-diagonal.  $\square$

#### 4. Projection Schemes for the Non-Abelian Case

In the previous section, we developed the time-reversible and volume-preserving projection scheme  $\Psi_h^\mu := P_b^\mu \circ \Phi_h \circ P_f^\mu$  described in (4) with block-diagonal matrix  $A$  for the Hamiltonian equations of motion

$$y' = f(y) = J^{-1} \nabla H(y) \quad \text{with} \quad y = (q, p)^T, \quad J = \begin{pmatrix} 0 & I \\ -I & 0 \end{pmatrix} \quad \text{and} \quad y(0) = y_0$$

in the Abelian case. Since we are interested in a scheme to solve the Hamiltonian equations of motion in the non-Abelian case of Lattice QCD, we adapt the projection scheme to this case here.

The Hamiltonian equations of motion in the non-Abelian case look similar to the Abelian one:

$$y' = f(y) = J^{-1} \nabla H(y), \quad y = (\{U\}, \{P\})^\top, \quad J = \begin{pmatrix} 0 & I \\ -I & 0 \end{pmatrix}. \quad (7)$$

In Lattice QCD, the configurations

$$\{U\} := (U_1, \dots, U_n)^\top \quad \text{and} \quad \{P\} := (P_1, \dots, P_n)^\top$$

consist of variables  $U_1, \dots, U_n$ , each an element of the special unitary Lie group  $SU(N)$ , and  $P_1, \dots, P_n$ , each a traceless and hermitian matrix of size  $N \times N$ . Now, we have to adapt the integration method  $\Phi_h$  to this special

type of differential equations on manifolds.

*Adaptation to Lie-group structure.* Applying the time-reversible and volume-preserving scheme (6) on the aforementioned equations of motion (7), we get a problem in the perturbation step:

$$U_1, \dots, U_n \in \text{SU}(N) \quad \rightarrow \quad U_1 + \mu A_{11} U_1, \dots, U_n + \mu A_{11} U_n \notin \text{SU}(N).$$

As the Lie group  $\text{SU}(N)$  is not closed with respect to addition, the results of the overall projection scheme will not be elements of the Lie group. A simple way out is the choice  $A_{11} = 0$ , i. e., the Lie group elements are not perturbed.

The variables  $\{P\} := (P_1, \dots, P_n)^\top$  are traceless and hermitian and, thus, elements of a linear space. Indeed,  $iP_1, \dots, iP_n$  are traceless and anti-hermitian or, in other words, elements of the special unitary Lie algebra  $\mathfrak{su}(N)$ . Here, we have no problems with the projection step:

$$iP_1, \dots, iP_n \in \mathfrak{su}(N) \quad \rightarrow \quad iP_1 + \mu A_{22} iP_1, \dots, iP_n + \mu A_{22} iP_n \in \mathfrak{su}(N).$$

*Scaling of momenta.* In addition to the choice  $A_{11} = 0$  made for meeting the Lie-group structure, we set  $A_{22} = I$  for a simple scaling of the momenta:

$$A = \begin{pmatrix} A_{11} & 0 \\ 0 & A_{22} \end{pmatrix} = \begin{pmatrix} 0 & 0 \\ 0 & I \end{pmatrix}. \quad (8)$$

The overall choice  $A_{11} = 0, A_{22} = I$  has two consequences: first, the elements  $U_1, \dots, U_n$  are never projected, they just occur in the inner one step integration scheme. Second, the variables  $P_1, \dots, P_n$  are just scaled by a simple factor  $1 + \mu$  in the perturbation step and the result of the intermediate one step integration scheme is then rescaled by a factor  $1/(1 + \mu)$ :

$$y_1 = \begin{pmatrix} \{U_1\} \\ \{P_1\} \end{pmatrix} = \begin{pmatrix} \Phi_h^U(\{U_0\}, (1 + \mu)\{P_0\}) \\ \frac{1}{1 + \mu} \Phi_h^P(\{U_0\}, (1 + \mu)\{P_0\}) \end{pmatrix}. \quad (9)$$

The Lie group structure is preserved –  $\Phi_h^U$  is still in the Lie group, and  $\Phi_h^P$  in the corresponding Lie algebra. Furthermore, the scheme (9) is still symmetric, time-reversible and volume-preserving. A big advantage is that there occurs no additional cost, except for the solution of the scalar equation

$$\tilde{g}(\mu) := g(y_h^{\mu^{opt}}) = H(y_h^{\mu^{opt}}) - H(y_0) = 0 \quad (10)$$

for the determination of  $\mu^{opt}$ .

## 5. Numerical Tests: Gauge Field in $SU(2)$

For the numerical test, we simulate a 2-dimensional gauge field in the special unitary Lie group  $SU(2)$  which is one of the most simple models in the field of Quantum Chromo Dynamics. Let us start with a short description of this model.

### 5.1. Gauge fields in the special unitary Lie group $SU(2)$

Given is a 2-dimensional lattice with periodic boundary conditions. At the end, we are interested in expectation values of type

$$\langle E \rangle = \sum_{\{U^i\}} p_i \cdot E(\{U^i\})$$

as defined in (1). This expectation value is composed of so-called links  $\{U\}$ , which are elements of the Lie group  $SU(2)$ , and define the connections between adjacent lattice points. For the Hybrid Monte Carlo method, fictitious momenta  $P_j$  with  $iP_j$  being an element of the Lie algebra  $\mathfrak{su}(2)$  are introduced at each lattice point  $j = 1, \dots, n$ . The Hamiltonian equations of motion

$$\dot{U}_j = \frac{\partial H(\{U, P\})}{\partial P_j} \quad \text{and} \quad \dot{P}_j = -\frac{\partial H(\{U, P\})}{\partial U_j}$$

have to be solved for each position  $j = 1, \dots, n$  on the lattice. The Hamiltonian, composed of the kinetic energy  $E_{\text{kin}}$  and the so-called Wilson gauge action  $S_G$ , reads

$$H(\{U, P\}) = E_{\text{kin}}(\{P\}) + S_G(\{U\}),$$

yielding the corresponding equations of motion

$$\dot{U}_j = P_j \cdot U_j \quad \text{and} \quad \dot{P}_j = -F(U_j, \{U\})$$

for each lattice point  $j = 1, \dots, n$ . Here, the equations for  $\dot{U}_j$  are differential equations on a manifold (Lie group) and the ones for  $i\dot{P}_j$  are differential equations in the linear space of a Lie algebra. The differential equation for  $P_j$  involves the corresponding link  $U_j$  itself and several adjacent lattice points, summarized by  $\{U\}$ , and is usually the more expensive part of the simulation.

At the end, the Hamiltonian equations of motion can be written in the compact notation (7)

$$\dot{y} = f(y) = J^{-1} \nabla H(y) \quad \text{with} \quad y = (\{U\}, \{P\})^\top, \quad J = \begin{pmatrix} 0 & I \\ -I & 0 \end{pmatrix}.$$

### 5.2. Numerical Tests

The numerical tests are performed on a lattice of size  $8 \times 8$  with periodic boundary conditions. In doing so, we start from already thermalized configurations and compute the mean value of 100 different configurations including statistical errors – which are in most cases so small that they can not be seen in the figures.

We have implemented the new projection scheme (9) in MATLAB. For the inner one-step scheme  $\Phi_h$ , we use the common Leapfrog scheme which has the advantage that it is explicit. The parameter  $\mu$  is determined via the scalar equation

$$\tilde{g}(\mu) = H(y_h^\mu) - H(y_0) = 0$$

mentioned in equation (10) using the bisection method.

Thereby, we investigate the step-size dependence of the following properties for the new projection scheme in comparison to the pure Leapfrog scheme without any projection: defect in the Hamiltonian, time-reversibility and volume-preservation. In this manner, we compute a whole trajectory of length  $\tau = 1$  using  $n = 1/h$  steps of step size  $h$ .

#### 5.2.1. Difference in the Hamiltonian

We start with a measurement of the difference  $\Delta H$  in the Hamiltonian before and after one step of the projection scheme (9), respective the Leapfrog method. In formulas, we have

$$\Delta H = H_{\text{new}} - H_{\text{old}} \quad \text{with} \quad H = E_{\text{kin}}(\{P\}) + S_G(\{U\}).$$

Since the Leapfrog scheme is a scheme of convergence order 2, it has an error of order  $h^3$  after one step. The difference  $\Delta H$  in the Hamiltonians is computed after a whole trajectory such that the error of the Leapfrog method in Figure 1 is of order  $h^2$ .

For the projection method, the accuracy just depends on the stopping criterion of the bisection method used for the determination of the parameter  $\mu$ . We can always choose the stopping criterion  $g(\mu)$  in such a way that the difference in the Hamiltonian is smaller than for the Leapfrog method.

#### 5.2.2. Time-Reversibility

We have seen in section 3.2 that the integration scheme  $\Psi_h$  has to fulfill the condition

$$\rho \circ \Psi_h \circ \rho \circ \Psi_h = id \quad \text{with} \quad \rho = \begin{pmatrix} I & 0 \\ 0 & -I \end{pmatrix}$$

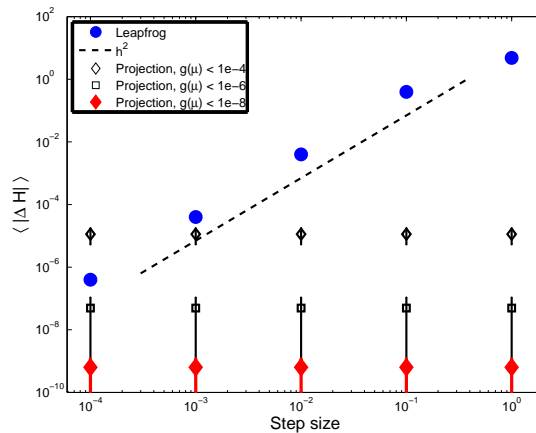


Figure 1: Absolute value of the difference in the Hamiltonian of 2 successive configurations  $\{U, P\}_{\text{old}}$  and  $\{U, P\}_{\text{new}}$  for Leapfrog method (blue circle) and projection method with constraint  $g(\mu)$  smaller than  $10^{-4}$  (black diamond),  $10^{-6}$  (black square) and  $10^{-8}$  (red diamond). Here, the mean value of 100 different configurations including statistical errors is given.

to be time-reversible. Here, the matrix  $\rho$  consists of blocks of size  $n \times n$  according to the dimensions of  $\{U\}$  and  $\{P\}$ . Thus, we compare the initial values  $\{U_0, P_0\}$  with the outcome of  $(\rho \circ \Psi_h \circ \rho \circ \Psi_h)(\{U_0, P_0\})$ . This comparison is done element by element and afterwards we take the mean of the absolute values of the differences in Figure 2. It can be seen that the differences of the Leapfrog and projection scheme are in the region of machine precision and coincide. Therefore, the numerical test validates the time-reversibility of our projection method.

### 5.2.3. Volume-Preservation

For the volume-preservation, we compute the absolute value of the determinant of the Jacobian of the system  $(\partial \Psi_h(\{U^0, P^0\}) / \partial \{U^0, P^0\})$ . Here, the Jacobian is attained via a one-sided numerical differentiation with fixed perturbation  $\varepsilon = 10^{-6}$ . In contrast to the Abelian case in  $\mathbb{R}^n$ , the computation of the Jacobian of a Lie-group/Lie-algebra is rather involved and follows the calculus derived in [11].

In Figure 3, we see a comparison between the volume-preserving Leapfrog method and the projection method with constraint  $g(\mu) < 10^{-8}$ . As the values coincide, the numerical test results validate the volume preservation

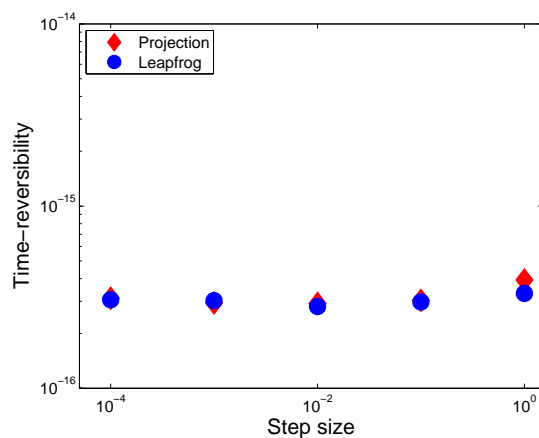


Figure 2: Time-reversibility: mean value of the absolute differences between the initial values  $\{U_0, P_0\}$  and the outcome of  $(\rho \circ \Psi_h \circ \rho \circ \Psi_h)(\{U_0, P_0\})$  for Leapfrog (blue circle) and projection method with constraint  $g(\mu)$  smaller than  $10^{-8}$  (red diamond).

of our projection scheme. The errors are due to the discretization errors introduced by numerical differentiation.

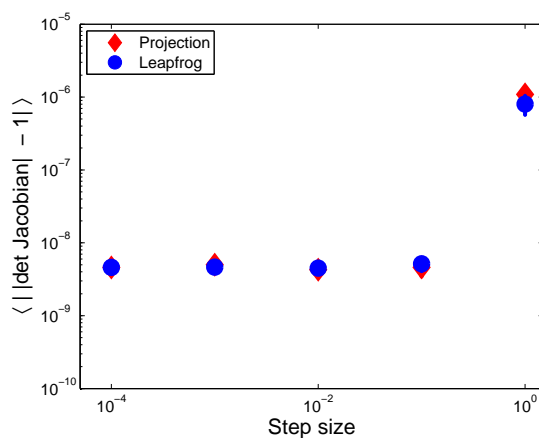


Figure 3: Volume-preservation: mean value of the absolute value of the determinant of the Jacobian of the system for Leapfrog (blue circle) and projection method with constraint  $g(\mu)$  smaller than  $10^{-8}$  (red diamond).

## 6. Conclusion and Outlook

Starting from symmetric projection, we constructed methods that are additionally time-reversible and volume-preserving, for the Abelian as well as the non-Abelian case. In the application of Lattice QCD, the new projection scheme has shown promising results within the Molecular Dynamics Steps of the Hybrid Monte Carlo method, validated by the numerical results obtained for a  $SU(2)$  gauge field: the difference in the Hamiltonian can be made arbitrarily small, thus avoiding rejection steps and allowing for large step sizes, at the prize of only solving one additional scalar equation to obtain the optimal value of  $\mu$ .

In a next step, we will investigate the autocorrelation behavior of the new projection scheme to check for statistically independent configurations needed in Lattice QCD. In addition, the projection scheme will be tested again for larger lattices, higher dimensions ( $SU(3)$  instead of  $SU(2)$ ) and more complex Hamiltonians including fermionic fields.

- [1] H. J. Rothe, *Lattice Gauge Theories: An Introduction*, Vol. 43 of *Lecture Notes in Physics*, World Scientific, 1992.
- [2] C. D. Thomas DeGrand, *Lattice Methods for Quantum Chromodynamics*, World Scientific Publishing Co Pte., 2006.
- [3] B. J. P. S. Duane, A. D. Kennedy, D. Roweth, *Hybrid Monte Carlo*, *Physics Letters B* 195 (1987) 216–222.
- [4] S. A. Gottlieb, W. Liu, D. Toussaint, R. L. Renken, R. L. Sugar, *Hybrid Molecular Dynamics Algorithms for the Numerical Simulation of Quantum Chromodynamics*, *Phys. Rev. D* 35 (1987) 2531–2542.
- [5] I. P. Omelyan, I. M. Mryglod, R. Folk, *Symplectic analytically integrable decomposition algorithms: classification, derivation, and application to molecular dynamics, quantum and celestial mechanics simulations*, *Computer Physics Communications* 151 (3) (2003) 272 – 314. doi:10.1016/S0010-4655(02)00754-3.
- [6] T. Takaishi, P. de Forcrand, *Testing and tuning new symplectic integrators for hybrid Monte Carlo algorithm in lattice QCD*, *Phys. Rev. E* 73:036706. arXiv:hep-lat/0505020v3.

- [7] J. C. Sexton, D. H. Weingarten, Hamiltonian evolution for the hybrid Monte Carlo algorithm, *Nucl. Phys. B*380 (1992) 665–678. doi:10.1016/0550-3213(92)90263-B.
- [8] M. Wandelt, M. Günther, F. Knechtli, M. Striebel, Symplectic partitioned Runge-Kutta methods for differential equations on Lie groups, *Applied Numerical Mathematics* 62 (2012) 1740–1748.
- [9] E. Hairer, Symmetric projection methods for differential equations on manifolds, *BIT Numerical Mathematics* 40 (2000) 726–734, 10.1023/A:1022344502818.  
URL <http://dx.doi.org/10.1023/A:1022344502818>
- [10] D. Shcherbakov, M. Ehrhardt, M. Günther, Symplectic and Time-Reversible Projection Methods for Hamiltonian Systems, submitted to *Journal of Computational and Applied Mathematics*.
- [11] M. Lüscher, Trivializing maps, the Wilson flow and the HMC algorithm arXiv:arXiv/0907.5491, doi:10.1007/s00220-009-0953-7.